

Spike output jitter, mean firing time and coefficient of variation

Jianfeng Feng and David Brown

Biostatistics Laboratory, The Babraham Institute, Cambridge CB2 4AT, UK

Received 17 June 1997, in final form 16 August 1997

Abstract. To understand how a single neurone processes information, it is critical to examine the relationship between input and output. Marsalek, Koch and Maunsell's study focused on output jitter (standard deviation of output interpike interval) found that for the integrate-and-fire (I&F) model this response measure converges towards zero as the number of inputs increases indefinitely when interarrival times of excitatory inputs (EPSPs) are normally or uniformly distributed. In this work we present a complete, theoretical investigation, corroborated by numerical simulation, of output jitter in the I&F model with a variety of input distributions and a range of values of number of inputs, N . Our main results are: the exponential distribution input is a critical case and its output jitter is independent of N . For input distributions with tails which decrease faster than the exponential distribution, output jitter converges to zero as discovered by Marsalek, Koch and Maunsell; whereas an input distribution with a more slowly decreasing tail induces divergence of output jitter. Exact formulae for mean firing time are also obtained which enable us to estimate the coefficient of variation. The I&F model with leakage is also briefly considered.

1. Introduction

Marsalek *et al* [24] have shown that output jitter (the standard deviation of the intervals between output spikes σ_{out}) in the integrate-and-fire (I&F) model converges to zero as the number of synaptic inputs (EPSPs) becomes large when EPSP interarrival time distributions are normal or uniform. Based upon extensive numerical simulations on more realistic neurones, they argue that this property provides one of the biophysical substrates necessary for exploiting the detailed timing information inherent in spike trains. However, a theoretically rigorous approach is lacking and furthermore we may ask ourselves: is this property universal in the sense that it is independent of input distribution, even in the simplest spiking model—the I&F model?

In this paper we carry out a theoretical study, corroborated by numerical simulation, of the relationship between input and spike output jitter. We find that there are three kinds of behaviour of σ_{out} and its relationship to the number of synaptic inputs.

- One is that discovered by Marsalek *et al* [24]. An exact relationship between input jitter and output jitter is given in the case when the input interarrival distribution follows the normal, uniform or truncated exponential distribution.

- A second is that σ_{out} diverges to infinity in the case when the input interarrival time distribution follows the Pareto distribution which indicates that each consecutive layer of spiking neurones will introduce more and more temporal jitter, compromising the ability of higher level neurones to respond sharply to a sensory input and rendering synfire assemblies [1, 2] difficult.

• A special case occurs when input timing is exponentially distributed; in this case σ_{out} remains constant as the number of inputs increases.

The important differences between exponential, Pareto and Gaussian distributions from the point of view of their effect on spike output jitter relate to tail length: the tail of the exponential distribution is $\exp(-x)$, the Pareto distribution $x^{-\alpha}$, $\alpha > 0$ (i.e. tending to zero more slowly as $x \rightarrow \infty$) and the Gaussian distribution is $\exp(-x^2/2)$ (tending to zero more quickly as $x \rightarrow \infty$).

For differently distributed inputs, the mean firing time is also exactly determined: either tending to infinity (the normal and exponential distribution) or to a constant (the uniform and truncated exponential distribution). Correspondingly there are different kinds of behaviour of the coefficient of variation C_v . We also consider the I&F model with leakage, in the average sense (see section 5).

The main tool we employ here is the statistical theory of extreme values which we have previously applied to other problems in neural computation [6, 10].

2. The I&F models

We begin with the simplest model of a spiking cell. In the I&F model each synaptic input instantaneously increments the membrane potential, V , positively or negatively, depolarizing or hyperpolarizing the membrane. Once V reaches a firing threshold V_{thre} , an output spike is generated and V is reset to V_{rest} , the resting potential. As in [24], for simplicity, the I&F unit is assumed to only receive inputs from N excitatory synaptic inputs of equal weight (EPSPs), a . Each synaptic input can be activated independently of the others. More precisely, the voltage $V(t)$ of the neurone satisfies

$$C\dot{V} = I(t) \quad (1)$$

with $V(0) = V_{\text{rest}}$, $I(t) = \sum_{i=1}^N a\delta(t - \xi_i)$ and independent identically distributed (i.i.d.) random sequence ξ_i , $i = 1, \dots, N$, C is the membrane capacitance. The solution of equation (1) is

$$V(t) = V_{\text{rest}} + \frac{1}{C} \sum_{i=1}^N aI_{\{\xi_i < t\}}$$

which means when $t = \xi_i$ the neurone receives an EPSP from the i th input. A typical set of parameters which match to slice recordings of regular spiking cells [28] are $V_{\text{rest}} = -73.6 \pm 1.5$ mV, $1/g_{\text{leak}} = 39.9 \pm 21.2$ M Ω , $C = \tau g_{\text{leak}}$, $\tau = 20.2 \pm 14.6$ ms. The absolute spike threshold V_{thre} was set 20 mV above V_{rest} , and a is a constant related to the size of a single EPSP. Recently [21] simultaneous intracellular recordings from pairs of pyramidal cells in cortical slice revealed a range of single-axon EPSPs from 0.05 mV to greater than 2 mV with a mean of 0.55 mV, which implies that we need about $N \sim 40$ EPSPs to trigger a spike.

Define $\xi = \inf\{t : V(t) > V_{\text{thre}}\}$. Again as in [24] we first suppose that when N (fixed but large) EPSPs arrive, an output spike is generated and so $\xi = \max\{\xi_1, \dots, \xi_N\}$. The output jitter is given by $\sigma_{\text{out}}^2 = E(\xi - E\xi)^2$. In section 6 we consider the more general case than $N - k$ EPSPs, for any given $N > k > 0$, are needed to trigger a spike.

3. Results for $k = 0$

For most commonly encountered random variable sequences, the distributions of their extreme value (maximum of the sequence) take the following form [18]

$$P(a_N(\xi - b_N) \leq x) \rightarrow G(x)$$

for constants a_N, b_N depending on specific distributions and G given in the appendix. Depending on the different forms of the distribution $G(x)$ they can be further divided into three types: type I, type II and type III (see the appendix).

3.1. Output jitter I: Gaussian and uniform distributions

Extreme value theory (see the appendix) tells us that the output jitter takes the form

$$\sigma_{\text{out}} = \sqrt{\langle(\xi - b_N)^2\rangle - \langle\xi - b_N\rangle^2} = \frac{1}{a_N} \sqrt{\int x^2 dG(x) - \left(\int x dG(x)\right)^2}. \quad (2)$$

In particular the output jitter of type I is thus[†]

$$\sigma_{\text{out}} = \frac{1}{a_N} \sqrt{\int_{-\infty}^{\infty} x^2 \exp(-e^{-x})e^{-x} dx - \left(\int_{-\infty}^{\infty} x \exp(-e^{-x})e^{-x} dx\right)^2} = \frac{1.277}{a_N}. \quad (3)$$

Under the condition that $\xi_i, i = 1, 2, \dots$, are i.i.d. random variables and normally distributed[‡] we have the following equation

$$\sigma_{\text{out}} = \frac{1.277}{\sqrt{2 \log N}}.$$

The mean of ξ , the average firing time of the neurone is $b_N \sim \sqrt{2 \log N}$. As observed by Marsalek *et al* [24] the firing time is delayed to b_N and the jitter is reduced. The relationship between input jitter σ_{in} and output jitter is

$$\frac{\sigma_{\text{out}}}{\sigma_{\text{in}}} = \frac{1.277}{\sqrt{2 \log N}}. \quad (4)$$

Note that constant 1.277 is universal for type I distributions.

The behaviour of output spike jitter of the uniform distribution is

$$\sigma_{\text{out}} = \frac{1}{N} \sqrt{\int_{-\infty}^0 x^2 \exp(x) dx - \left(\int_{-\infty}^0 x \exp(x) dx\right)^2} = \frac{1}{N} \quad (5)$$

which tends to zero faster than in the case of the Gaussian distribution. Unlike the normal distribution case the firing time becomes exact, at $t = 1$. The relationship between input jitter and output jitter is (see [24])

$$\frac{\sigma_{\text{out}}}{\sigma_{\text{in}}} = \frac{2\sqrt{3}}{N}. \quad (6)$$

The above two cases have been considered in [24] and our results coincide with theirs. In section 3.2 we consider output jitter for other distributions.

[†] The constant 1.277 is obtained from our numerical simulation (see figure 2).

[‡] This is not a sound assumption since we require $\xi_i \geq 0, i = 1, \dots, N$. However, for a comparison with numerical results of the same model in [24] we consider this case first. In section 3.2 we take into account more biologically plausible situations.

3.2. Output jitter II: Pareto, exponential and truncated exponential distribution

Very different behaviour is observed for type II random variables (the Pareto distribution with distribution function $1 - x^{-10/3}$, see the appendix). In this case we see that output jitter tends to infinity given by

$$\sigma_{\text{out}} = N^{0.3} \sqrt{\int_0^{\infty} 3x^{-2} \exp(-x^{-3}) dx - \left(\int_0^{\infty} 3x^{-3} \exp(-x^{-3}) dx \right)^2}$$

but with

$$\sigma_{\text{in}} = \sqrt{7}/4.$$

Let $c_1 = \sqrt{\int_0^{\infty} 3x^{-2} \exp(-x^{-3}) dx - \left(\int_0^{\infty} 3x^{-3} \exp(-x^{-3}) dx \right)^2}$. Then the relationship between input jitter and output jitter is given by† (see figure 2)

$$\frac{\sigma_{\text{out}}}{\sigma_{\text{in}}} = N^{0.3} c_1 \frac{4}{\sqrt{7}}.$$

A comparison of type I and type II distributions may give us the following impression. The Gaussian distribution with a distribution density $\exp(-x^2/2)$ decreases to zero exponentially and so the maximum of a sequence tends to infinity relatively slowly, i.e. with a small variance; whereas the Pareto distribution with a density $\alpha x^{-\alpha-1}$ goes to zero as a power (and hence much more slowly) and then the maxima become more spread. Nevertheless the behaviour of output jitter is more subtle as we discover in the following situations.

It is generally believed that for many neuronal systems ξ_1 is effectively exponentially distributed and so the distribution tail will tend to zero exponentially, which in turn is thought to imply shrinkage in output jitter with respect to input jitter. The shrink rate a_N depends on the specific distribution with a universal constant 1.277. But the exact picture is: for exponentially distributed ξ_1 we have $a_N = 1$, $b_N = \log N$ and thus the following equation holds

$$\frac{\sigma_{\text{out}}}{\sigma_{\text{in}}} = 1.277. \quad (7)$$

The firing time has a mean delay of $t = b_N$, but output jitter is constant, i.e. independent of N !

For a biological system there are physical limits, and so it is for the distribution of interarrival times of EPSPs. This means a further restriction on the distribution of timing can be introduced: a truncated exponential distribution, i.e. a random variable with distribution function $F(x) = K(1 - e^{-x})$ for $0 \leq x \leq x_F$. This results in type III limiting behaviour with

$$a_N = \frac{N}{e^{x_F} - 1} \quad b_N = x_F \quad \alpha = 1. \quad (8)$$

The relationship between output and input jitter is given by

$$\frac{\sigma_{\text{out}}}{\sigma_{\text{in}}} = \frac{e^{x_F} - 1}{N\sigma_{\text{in}}} \quad (9)$$

with $\sigma_{\text{in}}^2 = (K + 2e^{-K} - Ke^{-K} + 2e^{-K} - K^2e^{-K} - 2K^3e^{-K} - e^{-2K} - 2Ke^{-2K} - K^2e^{-2K})/K^2$. For synchronous firing of neurones, this is appropriate behaviour in the sense that the firing

† We take $c_1 = \frac{1}{1.4}$ obtained from our numerical simulation, see figure 2.

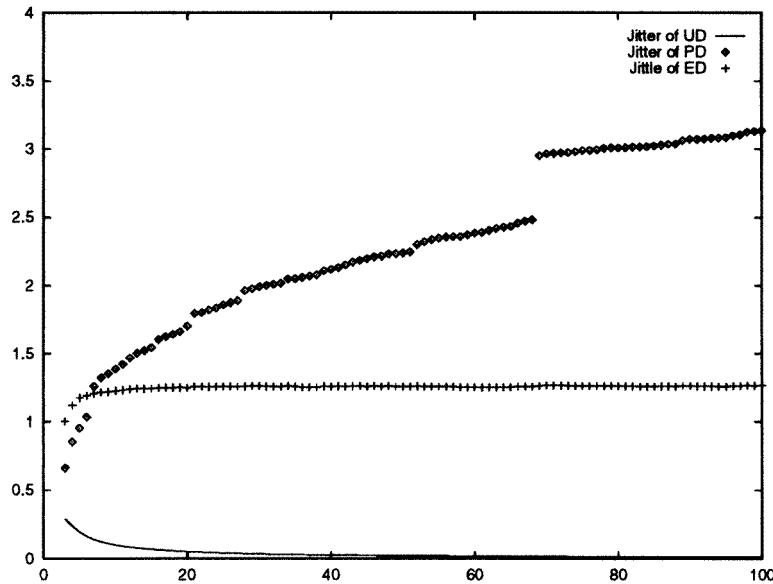


Figure 1. The output jitter versus N when input interarrival times follow a Pareto distribution, exponential distribution and uniform distribution (indicated PD, ED and UD respectively). The exponential distribution is the critical case with constant jitter; the fast decreasing distribution tail of the uniform distribution ensures output jitter converges towards zero, whereas the slow decay of distribution tail (Pareto) causes divergence of output jitter.

Table 1.

Distribution	Output jitter	Mean firing time
Gauss	$1.277/\sqrt{2 \log N}$	$\sqrt{2 \log N}$
Pareto ($\alpha = \frac{10}{3}$)	$N^{0.3}/1.4$	$1.3N^{0.3}$
Uniform	$1/N$	1
Exponential	1.277	$\log N$
Truncated exponential	$(e^{x_F} - 1)/N$	x_F

time becomes more and more precise, with output jitter decreasing at a rate of order $1/N$, similar to the uniform distribution.

We are now in a position to analyse the relationship between output jitter and input distribution. The exponential distribution is the critical case, with constant output jitter. The fast decreasing distribution tail of the truncated exponential distribution ensures that output jitter converges to zero. On the other hand, a slow decay like the Pareto distribution causes divergence of output jitter (see figure 1).

We summarize our results in the following theorem.

Theorem 1. In the I&F model, the mean and standard deviation of the output interspike interval distributions are as in table 1[†].

[†] See the next section for an estimation of constants.

3.3. C_v of output interspike intervals

In recent discussions of rate or timing coding of neural computation [14, 15, 22, 23, 25, 26], many people have paid attention to the coefficient of variation. The coefficient of variation (C_v) of output interspike intervals, defined as the standard deviation divided by the mean interspike interval, has been considered by several authors [31, 27] for the I&F model as well. Here as a simple consequence of our previous results we have the following ranges of C_v .

- Pareto: $0.5 < 1/(1.4 \times 1.3) < 1$ (a constant).
- Uniform: $1/N$ (tends to zero).
- Exponential: $1/\log N$ (tends to zero).
- Truncated exponential: $(e^{x_F} - 1)/(x_F N)$ (tends to zero).

4. Numerical results

In this section we present numerical simulations to confirm our theoretical results. Random numbers are generated using the NAG library and for each integer N ($= 3, \dots, 10\,000$) we average 10 000 times to obtain a single estimate of $\langle \sigma_{\text{out}} \rangle$. Three distributions: the exponential, uniform and Pareto distributions, are used in our simulations.

As predicted using our theoretical results we have the following.

- Output jitter of exponentially distributed EPSPs stays constant. This constant is universal for all type I distributions, equal to 1.277.

- For the uniform distribution the decreasing rate of its output jitter is $1/N$. Numerical results perfectly fit the theoretical formula.

- We set $\alpha = \frac{1}{0.3}$ in the Pareto distribution (see the appendix). The behaviour of output jitter of the Pareto distribution is substantially different from the above two cases: in the numerical simulations the effects of sampling variation on the estimates of mean and variance are still evident even after we base each estimate on 10 000 simulations for each value of N , although globally the numerical values are close to the theoretical ones. The oscillations in the sample curves occur because in the simulation experiments, to save computing time, the estimates for i synaptic inputs are obtained by supplementing the EPSPs underlying the estimates for $i - 1$ inputs with an additional randomly generated EPSP. From the numerical results we approximately estimate the constant c_1 in the previous section.

Now let us turn to numerical results for mean firing time. Since we are not able to estimate theoretically the mean firing time for the Pareto distribution, we simply estimate it numerically. It is found that $1.3N^{0.3}$ fits well. Remembering that output jitter of the Pareto distribution diverges to infinity and that in our numerical simulations the effects of sampling variation were apparent in the form of oscillations about the expected curve as shown in figure 2, it is at first sight surprising that the mean firing time diverges to infinity smoothly. Nevertheless, we might expect estimates of the mean to be much better behaved since they are dependent on only the first and not higher-order moments.

To fully understand the numerical results a few words on the difference between the Pareto distribution and the Gaussian distribution are needed. We are familiar with Gaussian distributions, which are also called ‘normal’ curves, and encountered frequently as sampling distributions of statistics (e.g. sample mean) that approach normality for large sample sizes, behaviour which is called asymptotically normal. The means and variances of these distributions are finite well defined values. However, these distributions are a subset of a much larger class of distributions that are called ‘stable distributions’, after Lévy [3]. Stable distributions have the property that the distribution of linear combinations of two

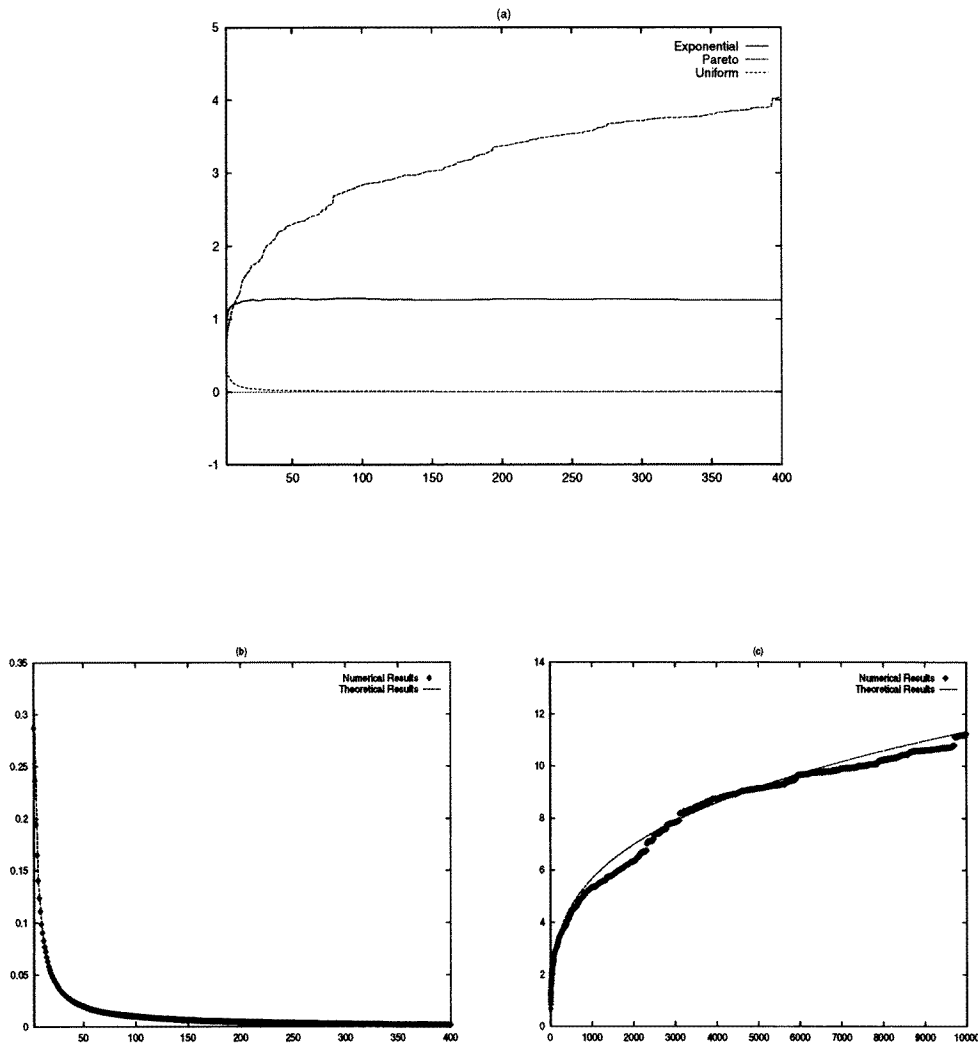


Figure 2. Numerical results of output jitter (σ_{out}) for different input distributions versus number of inputs. The exponential distribution is the critical case. (a) Output jitter is sensitive to input timing distribution. For exponentially distributed inputs, output jitter is constant, for the Pareto, output jitter diverges to infinity (replotted in (c)) and for the uniform output jitter converges to zero (replotted in (b)). (b) Output jitter of the uniform distribution versus number of inputs. Numerical results and theoretical estimate (see equation (5)) fit perfectly well. (c) Output jitter of the Pareto distribution versus the number of inputs. Note that there are always oscillations, although we have averaged over 10000 times of simulation at each value of N . Theoretical results show the theoretical curve $N^{0.3/1.4}$.

independent variables has the same shape as the original distribution. Stable distributions can have moments that are either finite or infinite. Gaussian distributions are stable distributions with finite mean and finite variance. These properties satisfy the conditions of the central limit theorem, which means that as more experimental data are analysed, the mean is determined with increased precision. There are also stable distributions with infinite variance or higher-order moments, which we call Lévy stable [20]. The property that the

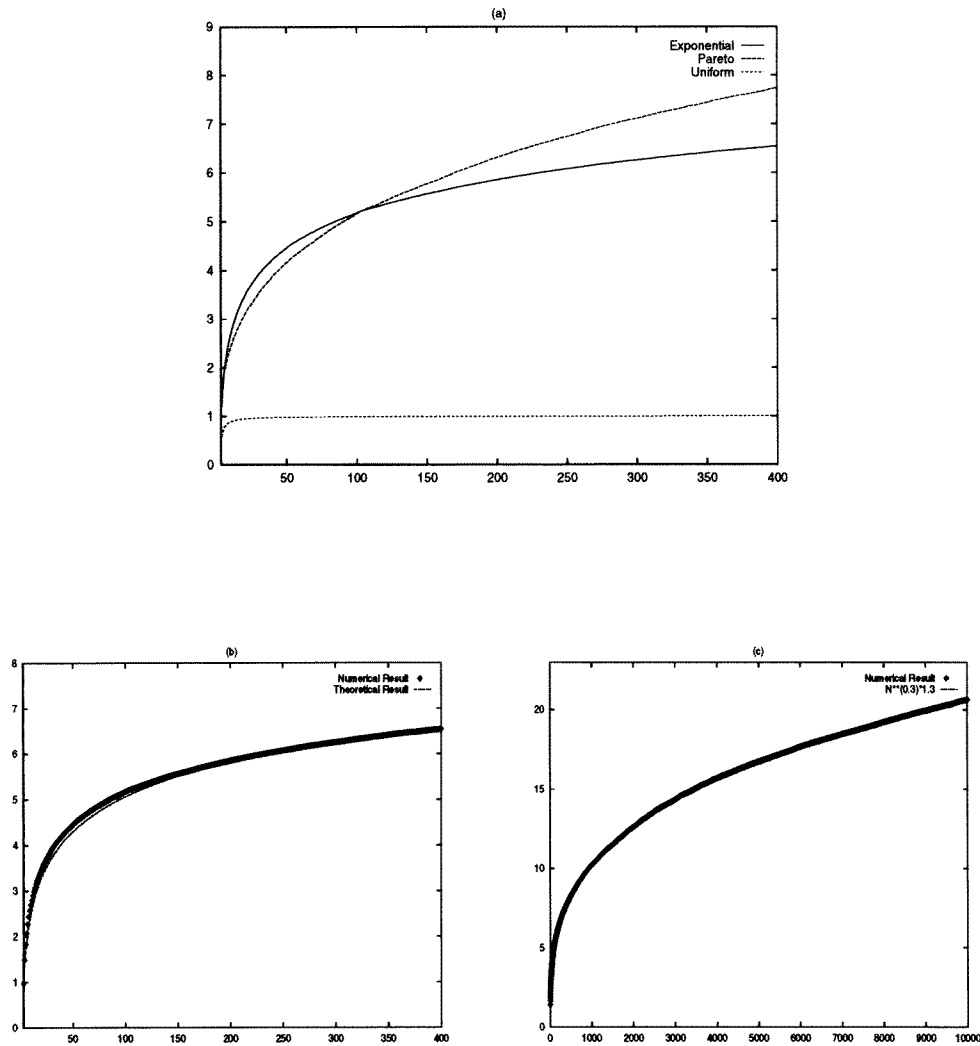


Figure 3. Numerical results of mean firing time of different distributions versus the number of inputs. For uniformly distributed inputs, mean firing time is constant (trivial). (a) The mean output firing time is sensitive to the input timing distribution. For exponential and Pareto inputs, the mean diverges to infinity (replotted in (b) and (c)). (b) Mean of the exponential distribution versus the number of inputs. Numerical results and theoretical estimate (see equation (5)) fit well as N is large. (c) Mean of the Pareto distribution versus number of inputs. Fitted curve is $1.3N^{0.3}$.

second-order moment is infinite means that this type of distribution does not satisfy the conditions of the central limit theorem in its usual form; indeed the variance of the linear combination, $\sum c_i X_i$, of independent variables such that $\sum c_i = 1$ can be the same as that of the distribution of each contributing random variable. Thus, as more experimental data are analysed, the precision of the determination of the mean does not improve. (See [3, pp 165–73] for a more theoretically oriented discussion on stable distributions and Lévy–Pareto distributions.)

A few words on proving whether a given set of data follows a distribution with a long tail

[11], where the tail of a distribution tends to zero geometrically (e.g. Pareto distribution), or with a short tail, where the tail of the distribution tends to zero exponentially (e.g. Gaussian, exponential or uniform distribution). With large data sets, trying to fit a traditional (short tail) distribution to a ‘truly’ long-tail distribution is equivalent to approximating a hyperbolically decaying function by a sum of exponentials. Although always possible, the number of parameters needed will tend to infinity as the sample size increases. Thus, long-tail distributions become a necessity from the point of view of parsimonious modelling of large data sets that exhibit the so-called ‘Joseph effect’ [20]. On the other hand, given a finite set of data, it is in principle not possible to decide whether the distribution is long tailed or not. For finite sample sizes, distinguishing between long and short tails is, in general, problematic and empirical studies of a single data set can result, therefore, in very different conclusions, depending on the statistical methods used. There has recently been considerable progress in developing a theory of statistical inference for long tailed distributions. While many problems remain unsolved, for some commonly encountered situations suitable statistical methods are now sufficiently well understood to be used in a larger class of data analyses (see for example [29]).

5. The model with leakage

It is well known that depolarizations do not persist forever, but that perturbations of membrane voltage tend to decay towards the resting potential. The I&F model with leakage can be expressed in the following way [16]

$$C\dot{V} = -g_{\text{leak}}V + I(t). \quad (10)$$

The solution of equation (10) is

$$V(t) = V_{\text{rest}} + \frac{1}{C} \sum_{i=1}^N \exp((\xi_i - t)/\tau) a I_{\{\xi_i < t\}}. \quad (11)$$

Note that in this case the actual number N of EPSPs which can activate a spike depends on each realization of ξ_i , $i = 1, 2, \dots$ and cannot be determined *a priori*.

Suppose that in the case of no leakage we need N_0 EPSPs to trigger a spike, then due to leakage, to acquire enough charge to emit a spike more EPSPs are needed. Let us first estimate how many EPSPs will trigger a spike in the leakage case. We confine ourselves to the normal distribution first. From the discussion of the previous section: the N th EPSP comes at a time which does not vary much at $\xi \sim \sqrt{2 \log N}$ for N large. Taking expectation on both sides of equation (11) we have

$$\langle V(\xi) \rangle = V_{\text{rest}} + \frac{\langle e^{\xi/\tau} \rangle a N}{C \exp(\sqrt{2 \log N}/\tau)}.$$

Let $(\langle V(\xi) \rangle - V_{\text{rest}})C/a = N_0$ then N_1 is given by

$$N_0 = \frac{\exp(1/(2\tau^2))N_1}{\exp(\sqrt{2 \log N_1}/\tau)}. \quad (12)$$

On average, N_1 EPSPs trigger a spike; σ_{out} reaches the value obtained at $N = N_0$ without leakage at $N = N_1 > N_0$ in its presence.

We employ numerical simulations to check the accuracy of our estimation. Taking $C = 1$, $a = 0.5$ mV and $\langle V(\xi) \rangle - V_{\text{rest}} = 20$ mV, $\tau = 20.2$ ms (see section 2 for the range

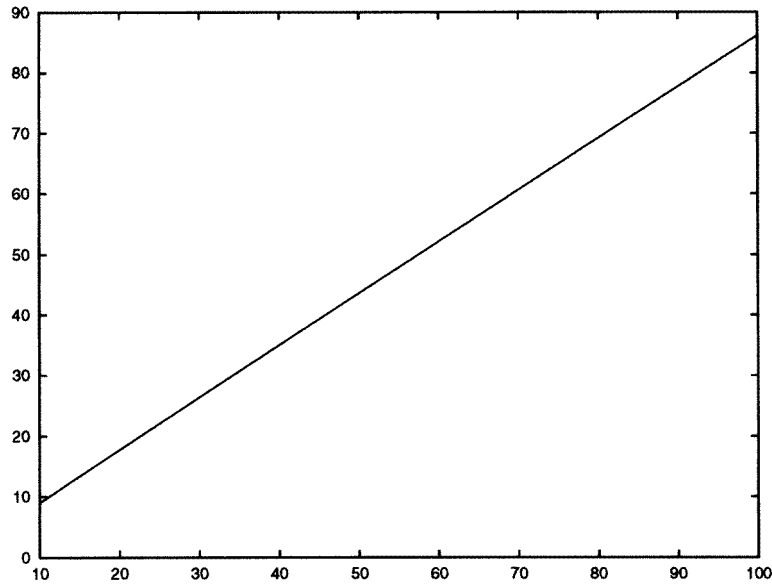


Figure 4. N_0 versus N_1 when $N_0 = 40$, N_1 is about 47.

of these parameters) we have $N_0 = 40$. From equation (12) (see figure 4) we see that N_1 is about 47. In terms of equation (11) we simulate

$$A = \sum_{i=1}^{47} \exp((\xi_i - t)/\tau) I_{\{\xi_i < t\}}$$

with $t = \sqrt{2 \log N_1}$ as mentioned above. We find that $A = 40.9 \sim N_0$ with a standard deviation of 0.4. This coincidence can be verified in terms of the law of large numbers as well. Hence N_1 of equation (12) gives a quite reasonable estimate of the average number needed to trigger a spike in the presence of leakage, which, in conjunction with results in the previous sections, enables us to reasonably assess other quantities such as the CV, output jitter and mean firing time of the model.

Analogous arguments can be applied to the situation in which EPSP emission follows distributional forms other than the Pareto distribution since the variance of ξ then becomes large.

6. More realistic models

One of the restrictions of the model that we considered in the previous section is that the neurone fires if and only if all N EPSPs arrive. What happens if $N - k$ EPSPs, for any given $0 < k < N$, are needed to trigger a spike?

For $k = 0, 1, \dots$, denote $\xi^{(k)} = \xi_{N_E - k}$ as the k th largest value of the sequence $\xi_1, \xi_2, \dots, \xi_{N_E}$. We have the following lemma.

Lemma 1 ([18]). For each $k = 0, 1, 2, \dots$,

$$P(a_N(\xi^{(k)} - b_N) \leq x) \rightarrow G(x) \sum_{s=0}^k \frac{(-\log G(x))^s}{s!} \quad (13)$$

where a_N, b_N and $G(x)$ depending on the input distributions are given in the appendix.

Table 2. A summary of results.

Distribution	Output jitter/input jitter	Mean firing time	Coefficient of variation
Gauss	converges towards zero	tends to infinity	
Pareto	diverges to infinity	diverges to infinity	between 0.5 and 1 ($\alpha = \frac{10}{3}$)
Uniform	converges towards zero	tends to a constant	tends to zero
Exponential	is constant	tends to infinity	tends to zero
Truncated Exponential	converges towards zero	tends to a constant	tends to zero

Denote

$$\bar{G}(x) = G(x) \sum_{s=0}^k \frac{(-\log G(x))^s}{s!}$$

we have, according to lemma 1, that

$$\sigma_{\text{out}} = \frac{1}{a_N} \sqrt{\int x^2 d\bar{G}(x) - \left(\int x d\bar{G}(x) \right)^2}. \quad (14)$$

Comparing equation (2) with equation (14), we conclude that all results on σ_{out} in sections 3 and 4 are true for the case considered in this section with a different contractive or expanding constant $\sqrt{\int x^2 d\bar{G}(x) - \left(\int x d\bar{G}(x) \right)^2}$ depending on k .

7. Discussion

In an attempt to fully understand the exact relationship between output jitter and input jitter for the I&F model, we have analytically derived a number of results. These tell us that there are different types of behaviour for output jitter, mean firing time and coefficient of variation depending on the nature of EPSP interarrival time distribution. We summarize our results in table 2.

Although our previous discussion and biological findings could be said to favour the hypothesis that EPSPs are emitted in a random fashion subjected to the truncated exponential distribution, it is known that the magnitude of EPSPs varies greatly, depending on their location on the dendritic tree [17], quantal fluctuations, etc. Neuronal responses are also very different. For example magnocellular vasopressin hypothalamic neurones fire without apparent correlation from neurone to neurone, whereas oxytocin neurones also found in the hypothalamus are strongly organized to fire together at certain times [13]. Our results in this paper present the whole spectrum of types of behaviour of output jitter which provides a prototype for further tests on assumptions of information processing in single neurones. Results in this paper indicate that a neurone is in a critical position if input EPSPs are exponentially distributed; and a perturbation of the tails of the distribution can result in a change of its output jitter—from convergence to divergence—and consequently its ability in information processing.

The possibility that the brain might use higher-order statistics has been pointed out from a theoretical view point before [19]. Our results also support the idea that neurones can be either a natural signal amplifier (when output jitter converges) or a signal attenuator (when output jitter diverges) dependent on the higher-order statistics of input signals.

A few words about our approach using the statistical theory of extreme values are needed. It seems that the power of extreme value theory in neural computation has not yet been fully realized. In previous papers [8–10, 7] we developed a theory related to extreme values in other classes of neurodynamics. In [6], we applied extreme value theory to some challenging problems in neural computation, such as the capacity of the Hopfield model, learning curves of perceptron learning etc. In this paper, we have seen how this theory can be exploited in relation to neurones as threshold devices utilizing the fact that when membrane potential exceeds a threshold, in other words takes an extreme value, the neurone fires. Hence, at least theoretically when confronting some complex nonlinear phenomena arising in neural computation, this well-developed theory—the statistical theory of extreme values—can help us to understand and model some important phenomena, as we have demonstrated previously and in this paper.

Finally, we point out here that although the original motivation in this paper for considering the I&F model is the modelling of a single neurone it should be mentioned that the model is grossly idealized. Despite the unphysiological nature of the model, it is useful because the model can be analysed completely thereby providing a standard with which to compare other models and also real nerve cells [5]. The real situation in biological systems is far more complex than we discuss here. Thomson and his colleagues (see for example [30] and references therein) carried out *in vitro* experiments to characterize the activity-dependent properties of synaptic transmission and these properties have been included in the I&F model of [4]. As mentioned above, leakage is not catered for in most of our results, although we do provide an assessment of its effect. The detailed mechanisms of IPSPs have also not been included, although in some biological experiments these can be blocked. The I&F model with exclusively excitatory inputs has also been employed to model a wide variety of phenomena in physiology: for example the micturition reflex, the mechanical ventilation of cats which exhibits chaotic behaviour, and also in the context of circadian rhythms etc (see [12] for a review). Furthermore in some neuronal systems excitatory cells are known to vastly outnumber inhibitory neurones. For example, 85–90% of cortical cells are estimated to be excitatory [2, p 53]. In these cases a model based on excitatory synaptic input might form a useful approximation. The I&F model has also been the subject of many recent neural modelling studies [27, 31, 24] and has been shown to match experimental neuronal spike trains well (e.g. [11, 32]). When particularly focusing on stochastic synaptic input, the I&F model is a yardstick for comparison with more complex models. A great strength in this context is that it is more analytically tractable than biologically more realistic models; results of the type presented here are not available for more realistic models. Complications such as different levels of inhibitory input and leakage analysed using simulation will be presented elsewhere (e.g. [5]). In any case, after many years' modelling single neurones, in the face of the diverse complexities of real neurones, the minimum combination of elements needed for a model to reflect key properties of the real thing remains a matter of conjecture.

Acknowledgments

We are grateful to W B Fu for his valuable comments on an earlier version of this article. The paper was partially supported by a BBSRC LINK programme and an ESEP of the Royal Society.

Appendix. Behaviours of extreme values

All materials presented here can be found in [18]. There are three types of behaviour for the extreme value of a random sequence.

Type I:

$$G(x) = \exp(-e^{-x}) \quad -\infty < x < \infty.$$

The normal distribution is a special case with

$$\begin{cases} a_N = (2 \log N)^{1/2} \\ b_N = (2 \log N)^{1/2} - \frac{1}{2}(2 \log N)^{-1/2}(\log \log N + \log 4\pi). \end{cases} \quad (\text{A1})$$

Type II:

$$G(x) = \begin{cases} 0 & x \leq 0 \\ \exp(-x^{-\alpha}) & \text{for some } \alpha > 0 \quad x > 0. \end{cases}$$

The Pareto distribution with distribution function $F(x) = 1 - Kx^{-\alpha}$, $x \geq K^{1/\alpha}$, $K > 0$, $\alpha > 0$ is a candidate of this type of behaviour with $a_N = (KN)^{-1/\alpha}$, $b_N = 0$. For simplicity of notation we take $K = 1$ and $\alpha = \frac{10}{3}$ in our following discussion.

Type III:

$$G(x) = \begin{cases} \exp(-(-x)^\alpha) & \text{for some } \alpha > 0 \quad x \leq 0 \\ 1 & x > 0. \end{cases}$$

The uniform distribution on $[0, 1]$ is of this type with $\alpha = 1$, $a_N = N$ and $b_N = 1$.

Various necessary and sufficient conditions are known—involving the ‘tail behaviour’ $1 - F(x)$ as x increases—for each type of limit, where $F(x)$ is the distribution function of ξ_1 . Here is an example. Let $x_F = \sup\{x; F(x) < 1\}$. Then ξ_i , $i = 1, \dots, N$ belong to each of the three types if and only if:

type I: there exists some strictly positive function $g(t)$ such that $\lim_{t \rightarrow x_F} (1 - F(t + xg(t)))/(1 - F(t)) = e^{-x}$ for all x ;

type II: $x_F = \infty$ and $\lim_{t \rightarrow \infty} (1 - F(tx))/(1 - F(t)) = x^{-\alpha}$, $\alpha > 0$, for each $x > 0$;

type III: $x_F < \infty$ and $\lim_{h \rightarrow 0} (1 - F(x_F - xh))/(1 - F(x_F - h)) = x^\alpha$, $\alpha > 0$, for each $x > 0$.

References

- [1] Abeles M 1982 *Local Cortical Circuits: An Electrophysiological Study* (New York: Springer)
- [2] Abeles M 1991 *Corticonics* (Cambridge: Cambridge University Press)
- [3] Feller W 1966 *An Introduction to Probability Theory and its Applications* (New York: Wiley)
- [4] Abbott L F, Varela J A, Sen K and Nelson S B 1997 Synaptic depression and cortical gain control *Science* **275** 220–3
- [5] Feng J and Brown D 1997a Impact of temporal variation and the balance between excitation and inhibition on the output of the integrate and fire model *Neural Comput.* submitted
- [6] Feng J and Brown D 1997b Generalization errors of the simple perceptron *J. Phys. A: Math. Gen.* accepted
- [7] Feng J and Brown D 1998 Fixed point attractor analysis for a class of neurodynamics *Neural Comput.* **10** 189–213
- [8] Feng J, Pan H and Roychowdhury V P 1996 On neurodynamics with limiter function and Linsker’s developmental model *Neural Comput.* **8** 1003–19
- [9] Feng J, Pan H and Roychowdhury V P 1997 Linsker-type Hebbian learning: a qualitative analysis on the parameter space *Neural Networks* **10** 705–20
- [10] Feng J and Tirozzi B 1995 An application of the saturated attractor analysis to three typical models *Lect. Notes Comput. Sci.* **930** 353–60

- [11] Gerstein G L and Mandelbrot B 1964 Random walk models for the Spike activity of a single neuron *Biophys. J.* **4** 41–68
- [12] Glass L and Mackey M C 1988 *From Clocks to Chaos: The Rhythms of Life* (Princeton, NJ: Princeton University Press)
- [13] Leng G and Brown D 1997 The origins and significance of pulsatility in hormone secretion from the pituitary *J. Neuroendocrinol.* **493** 493–513
- [14] Gray C M and McCormick D A 1996 Chattering cells: superficial pyramidal neurons contributing to the generation of synchronous oscillations in the visual cortex *Science* **274** 109–13
- [15] Hopfield J J 1995 Pattern recognition computation using action potential timing for stimulus representation *Nature* **376** 33–6
- [16] Knight B 1972 Dynamics of encoding in a population of neurons *J. Gen. Physiol.* **59** 734–66
- [17] Koch C 1997 Computation and the single neuron *Nature* **385** 207–10
- [18] Leadbetter M R, Lindgren G and Rootzén H 1983 *Extremes and Related Properties of Random Sequences and Processes* (New York: Springer)
- [19] von del Malsburg C 1981 The correlation theory of brain function *Internal Report* 81–2 (Goettingen: Max-Planck-Institute for Biophysical Chemistry)
- [20] Mandelbrot B B 1983 *The Fractal Geometry of Nature* (New York: Freeman)
- [21] Mason A, Nicoll A and Stratford K 1991 Synaptic transmission between individual pyramidal neurons of the rat visual cortex *in vitro* *J. Neurosci* **11** 72–84
- [22] Mainen Z F and Sejnowski T J 1995 Reliability of spike timing in neocortical neurons *Science* **268** 1503–6
- [23] Mainen Z F and Sejnowski T J 1996 Influence of dendritic structure on firing pattern in model neocortical neurons *Nature* **382** 363–6
- [24] Marsalek P, Koch C and Maunsell J 1997 On the relationship between synaptic input and spike output jitter in individual neurons *Proc. Natl Acad. Sci., USA* **94** 735–40
- [25] Sejnowski T J 1995 Time for a new neural code? *Nature* **323** 21–2
- [26] de Ruyter van Steveninck R R, Lewen G D, Strong S P, Koberle R, and Bialek W 1997 Reproducibility and variability in neural spike trains *Science* **275** 1805–8
- [27] Softky W and Koch C 1993 The highly irregular firing of cortical-cells is inconsistent with temporal integration of random EPSPs *J. Neurosci* **13** 334–50
- [28] Shadlen M N and Newsome W T 1994 Noise, neural codes and cortical organization *Curr. Opin. Neurobiol.* **4** 569–79
- [29] Stanley H E *et al* 1996 Scaling and universality in animate and inanimate systems *Physica* **231A** 20–48
- [30] Thomson A M 1997 Activity-dependent properties of synaptic transmission at two classes of connections made by rat neocortical pyramidal *J. Physiol.* **502** 131–47
- [31] Troyer T W and Miller K D 1997 Physiological gain leads to high ISI variability in a simple model of a cortical regular spiking cell *Neural Comput.* **9** 733–45
- [32] Tuckwell H C 1988 *Stochastic Processes in the Neurosciences* (Philadelphia, PA: Society for Industrial and Applied Mathematics)